Journal of Telecommunication, Electronic and Computer Engineering
ISSN: 2180 – 1843 e-ISSN: 2289-8131 Vol. 15 No. 3
jtec.utem.edu.my

A Proposed Frequency Selective Surface (FSS) using Bio-Inspired Element for Wi-Fi 6E Applications

Guilherme W. Pereira[1], Alexandre J. R. Serres[2], Georgina K. F. Serres[2], Jefferson C. e Silva[3] and Robson H. C. Maniçoba[4]
[1]*Computing Institute (IC), Federal University of Bahia (UFBA), Salvador, Bahia, Brazil*
[2]*Department of Electrical Engineering (DEE), Federal University of Campina Grande (UFCG), Campina Grande, Paraíba, Brazil*
[3]*Group of Telecommunications and Applied Electromagnetism (GTEMA), Federal Institute of Paraíba (IFPB), João Pessoa, Paraíba, Brazil*
[4]*Department of Science and Technology (DCT), State University of Southwestern Bahia (UESB), Jequié, Bahia, Brazil*
rhcmanicoba@uesb.edu.br

Article Info

Article history:
Received July 11th, 2023
Revised Aug 15th, 2023
Accepted Aug 23th, 2023

Index Terms:
Frequency Selective Surface
Polarization Independence
Rejection Bandwidth
Wi-Fi

Abstract

Recently bio-inspired elements with shapes or geometries found in nature have received special attention, both for applications in antennas and in electromagnetic filters, the unit cell of the proposed FSS consists of a modification in a bio-inspired shaped element. A single and multilayered band-stop Frequency Selective Surface (FSS), with polarization independence, is proposed to be used in frequency applications at 6.0 GHz (Wi-Fi 6E). In the industry, Wi-Fi 6E is the name that identifies those Wi-Fi devices that operate in the 6.0 GHz band, designed to improve efficiency and more capacity than previous standards. Band-stop frequency responses for the single and multilayer structures are presented. The simulated frequency responses show bandwidth values for inhibit transmission about of 1.75 GHz and 3.15 GHz, respectively for single and multilayer structures. Furthermore, good agreement between simulated and measured results is shown for the single bio-inspired FSS. The proposed FSS structure presents features that allow its use as an electromagnetic filter or its integration with microstrip antennas developed for applications in the same standard.

I. INTRODUCTION

Frequency Selective Surfaces (FSS) can be defined as properly designed surface structures, widely used as spatial filters in a range of telecommunications applications, such as Wi-Fi applications. These structures, a kind of periodic structure, can also be defined as 2D or 3 structure-array structures of identical elements on one side (or more sides, depending) of the dielectric structure layer. The elements used in its unit cell can be of conductive (metallic) patch type, aperture type, or an array of all-dielectric elements. FSS structures can exhibit band-pass, band-stop or even both characteristics that are interesting in the same structure (multi-band responses), depending on their behavior in terms of frequency response (that is, in certain frequency bands it acts as a band-stop filter and in others as a band-pass filter for the same structure), with the proposal for blocking electromagnetic waves in certain frequencies, which depends primarily on the type and the geometry of the structure in its unit cell [1-4].

FSS structures have received special attention from researchers over the years due to their widespread applications in the Telecommunication Engineering area and correlated areas. Such applications include band-stop and band-pass spatial filters, absorbers (absorptive FSS), artificial electromagnetic bandgap materials, used as superstrate of antenna or antenna array to enhance the directivity and gain [5-8].

The integration with antenna systems to act as radomes and subreflectors is one of the most important uses of FSS structures applications. The latter is widely used in applications to separate electromagnetic waves into different frequency bands.

An important problem in FSS theory is the question of operating bandwidth in the frequency response for the transmission or reflection characteristics. Generally, FSS structures formed by elements with a simple shape will produce a single resonance mode. It is possible to obtain FSS structures with multiband or wideband frequency responses by using different methods, for example, complex elements, combined-based elements, and multilayered structures. FSS structures with complex elements (spiral, fractal, bio-inspired, among others), polarization-independent, angular stability, and multiband or wideband characteristics, have received special attention [9-15].

In [16] a polarization-insensitive multilayer FSS structure on a glass substrate for shielding WLAN frequency bands from 2.4 GHz to 2.5 GHz and 4.98 GHz to 5.825 GHz,

allowing transmission cellular frequency bands at 900 MHz and 1.8 GHz with very low attenuation is proposed.

An ultra-compact absorptive FSS (AFSS) based on via structure, operating at 5.0 GHz Wi-Fi band is proposed in [17] to solve electromagnetic interference (EMI) and radio frequency interference (RFI) problems in mixed-signal systems. A highly miniaturized polarization selective surface (PSS) for dual-band Wi-Fi and WLAN applications using two independently tunable square loops is reported in [18]. The authors in [19] present an FSS structure designed to use in Wi-Fi applications as either a reject or pass band filter, the proposed structure consists of a combination of canonical elements (ring loops/slots).

A convoluted geometry used as an FSS unit cell with angular stability and independent polarization operation is used in [20] for dual-band applications at ISM and UNII bands. A combination of open and closed loop elements is presented in [21] for a dual-band FSS to block Wi-Fi signals at 2.45 GHz and 5.5 GHz, allowing the transmission of the signals outside of these bands.

An antenna application using FSS for bandwidth and gain enhancement for WLAN and WIMAX is proposed in [22]. The proposed structure is obtained by combining E and T-shaped radiating patches of antenna elements with a FSS under the modified ground plane. Already in [23], an antenna with dual-band, high-gain and linearly polarized using a defective FSS is proposed to use in Wi-Fi, Wi-Max and C-band applications.

Bio-inspired shaped elements have received special attention in telecommunications research. In [24] a microstrip antenna with leaf-shaped printed monopole element bio-inspired on the Inga Marganita leaves for ultra-wideband (UWB) applications is proposed. Bio-inspired wearable antennas are presented in [25], such as wearable monopole antenna bio-inspired in jasmine flower shape, wearable antenna bio-inspired in Bidens Pilosa plant shape, wearable antenna arrays bio-inspired in Inga Maritimus plant shape.

A bio-inspired FSS proposal is presented in [26], for this case, the element geometry used as the unit cell is inspired on the leaf of the Oxalis Triangularis plant and has a resonant frequency at 3.5 GHz.

Wi-Fi 6E can be defined, in the industry, as the name that identifies Wi-Fi device applications that operate in 6.0 GHz frequency band. With up to 1.2 GHz spectrum available, features and capabilities include higher performance, lower latency and faster data rate. Wi-Fi 6E utilizes the less congested 6.0 GHz band to enable high-bandwidth applications [27-28].

In this paper, a single and multilayer band-stop FSS with bio-inspired shaped elements is proposed. The shaped element is inspired by a modified four-leaf clover. The proposed FSS structure is developed in three steps. In the first one, a bio-inspired FSS single screen with four-leaf clover patch elements was designed. In the second step, a modification was made to the initial design of the element shape, this modification was responsible for a frequency adjustment for the proposed application. In the third step, two FSS screens (obtained in the first step) were cascaded separated by an air gap layer to improve the bandwidth behavior.

The proposed FSS structure using the bio-inspired element in the unit cell provides similar transmission characteristics for both X-polarized electric field (TE Mode) and for Y-polarized electric field (TM Mode) for a normal incidence, that is, polarization independence. This type of characteristic is due to the fact that the shape of the element, and consequently the structure, presents symmetry.

II. FSS STRUCTURE

The proposed FSS structure starts with the use of the bio-inspired four-leaf clover-shaped metallic patch element in its unit cell. The structure used in the work was based on the four-leaf clover proposed in [29] as an antenna element. The four-leaf clover-shaped geometry used in the FSS structure design was obtained using the Gielis formula [30] also known as superformula. This superformula allows obtaining various types of geometries or shapes and curves commonly found in nature, these patterns can be generated through equation 1. The initial pattern obtained can be seen in Figure 1. A modification was made to the pattern by removing the metallic layer (copper) in the shape of a semicircle at the ends of the four leaves of the structure with the following features: 1.79 mm arc, 3.55 mm high and 8.61 mm wide. This shaped element unit cell and its parameters can be seen in Figure 2.

$$r(\theta) = \left[\left|\frac{1}{a}cos\left(\frac{m}{4}\theta\right)^{n2}\right| + \left|\frac{1}{b}sin\left(\frac{m}{4}\theta\right)^{n3}\right|\right]^{-\frac{1}{n1}} \quad (1)$$

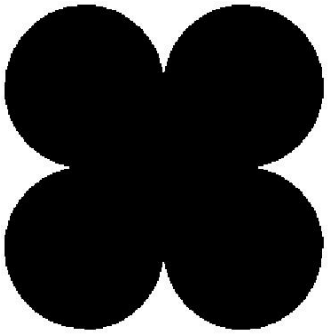

Figure 1. Initial pattern.

The development of this initial pattern shown in Figure 1 was made using the software Octave®, through the implementation of equation 1.

After obtaining the results for the initial structure, it was modified by inserting an open-type element in a circle shape. This subtle modification made the frequency response ideal for the proposed application.

The unit cell using a modified bio-inspired four-leaf clover metallic patch element is presented in Figure 3.

The structure shown in Figure 3 is identical to the structure shown in Figure 2 and its parameters, with the exception of the modification performed with the insertion of the aperture type element with a circle shape with parameter R = 4.0 mm.

The FSS structure is mounted on a dielectric substrate (a low-cost FR-4 substrate) with relative permittivity of 4.4 with dielectric loss tangent of 0.02 and the thickness dielectric substrate is 1.6 mm.

With the results obtained for the FSS structure using the modified bio-inspired elements, the multilayer structure was carried out. The cascade structure was obtained by coupling two identical FSS structures with modified bio-inspired elements separated by an air gap layer.

The periodicity considered for the construction of the unit cell in Fig. 1 was Tx = Ty = 30.44 mm. For the other parameters, the following values were used: the length X = 24.35mm, the cavity Y = 12.0 mm, and the cavity Z = 8.61 mm.

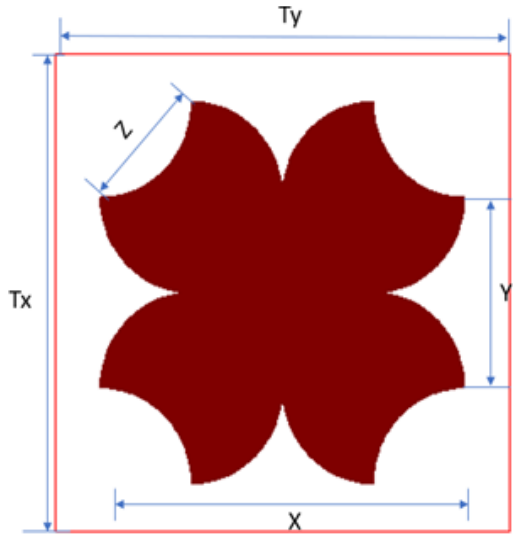

Figure 2. A bio-inspired initial shaped element unit cell.

This technique mentioned above is widely used as a solution to the problem-question of FSS bandwidth operation. The proposed multilayered bio-inspired FSS structure can be seen in Figure 4.

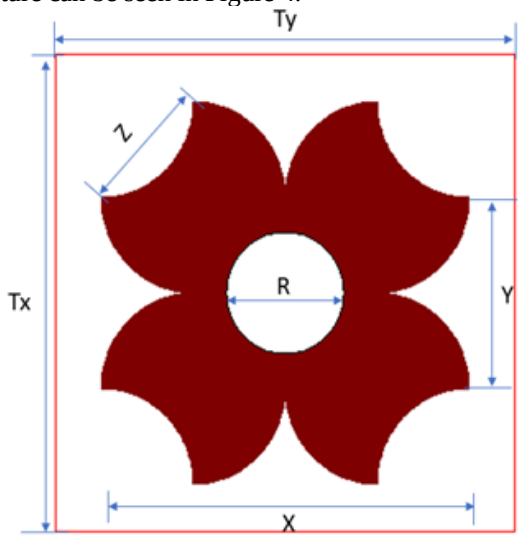

Figure 3. A modified bio-inspired element unit cell.

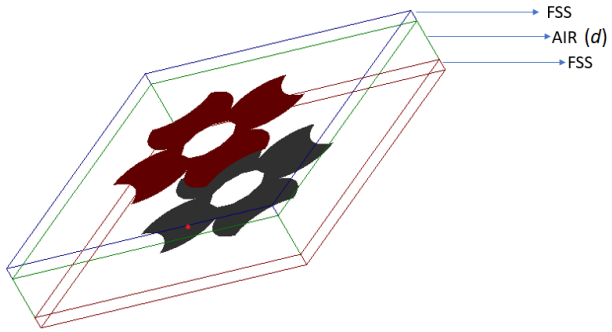

Figure 4. Multilayered FSS structure with a modified bio-inspired element.

Several tests were carried out with different values for the air gap layer, also interpreted as distance (*d*) between the two FSS structures.

III. RESULTS

The performance of the proposed single and multilayer bio-inspired FSS structures, in terms of transmission characteristics, was obtained using software based on the numerical technique Method of Moments (MoM) and using the Scattering Matrix Technique (one-mode interaction) for the cascaded FSS structure to perform a parametric analysis of the air layer effect between individual FSS structures.

Once the individual structure results for the transmission and reflection coefficients have been obtained, the interaction between the two structures can be accounted for by using the scattering matrix. This technique can be used for cascading between a number *N* of FSS structures, in the case presented here only two FSS were used. The cascaded structure is represented in Figure 5.

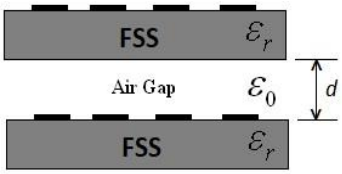

Figure 5. Cascaded FSS structure representation.

First, for each FSS sheet, we determine a 2 x 2 scattering matrix S, using [31]:

$$\overline{\overline{S_n}} = \begin{bmatrix} T_n\left(1-\frac{R_n^2}{T_n^2}\right) & \left(\frac{R_n}{T_n}\right)e^{j2kl_n} \\ -\left(\frac{R_n}{T_n}\right)e^{-j2kl_n} & \frac{1}{T_n} \end{bmatrix} \quad (2)$$

where,

$$l_n = d_1 + d_2 + \cdots + d_n \quad (3)$$

For the case previously described, shown in Figure 4 and represented in Figure 2, $l_n = d$, i.e. the thickness of the air layer (distance between the two FSS). The coefficients T_n and R_n are the transmitted (S_{21}) and reflected (S_{11}) coefficients obtained separately for the *n-th* structure. Using the one-mode interaction, the final results of the reflection and transmission coefficient for the cascading structure in Fig. 2 are [31]:

$$T = A - \left(\frac{BC}{D}\right) \quad (4)$$

$$R = -\left(\frac{C}{D}\right) \quad (5)$$

The coefficients (A, B, C, D), from the ABCD matrix, are calculated as:

$$\begin{bmatrix} A & B \\ C & D \end{bmatrix} = \overline{\overline{S_n S_{n-1}}} \ldots \overline{\overline{S_3}}\,\overline{\overline{S_2}}\,\overline{\overline{S_1}} \quad (6)$$

For the special case where N=2, that is, cascading two FSS, it can be obtained that:

$$T = \frac{T_1 T_2}{1 - R_1 R_2 e^{-j2kd}} \quad (7)$$

$$R = R_1 + \frac{T_1^2 R_2}{1 - R_1 R_2 e^{-j2kd}} e^{-j2kd} \quad (8)$$

The terms T_1, R_1 (S_{21}, S_{11}) are the transmission and reflection coefficients of FSS structure shown in Figure 3, respectively. Since we have identical structures in the composition of the multilayer structure, T_1=T_2 and R_1= R_2. The T and R terms are the transmission and reflection coefficients of the cascaded or multilayer FSS structure (Figure 4). The numerically simulated results, for the single FSS, are presented in Figures 6 – x.

As can be seen in Figure 6, the simulation of initial FSS with a bio-inspired four-leaf clover element generated a band-stop filtering that starts at 5.2 GHz and ends at 7.0 GHz, with resonant frequency at 6.3 GHz (-38.17 dB) resulting in a bandwidth of 1.8 GHz, for a -10 dB insertion loss reference level. It is also possible to observe, for this case,polarization independence (TE Mode and TM Mode with the same results).

Figure 7 shows the simulated results obtained, in terms of transmission characteristics and S_{11}, for a single-layer FSS structure with modified bio-inspired elements.

Observing Figure 7, it can be seen that the modification performed in Figure 2 and shown in Figure 3, led to a change in frequency response.

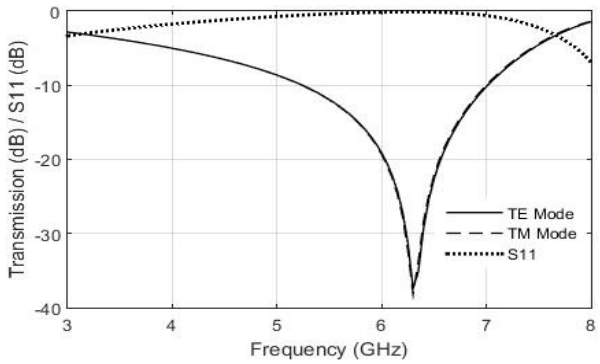

Figure 6. Simulated transmission coefficients for TE mode and TM mode and S_{11} for the proposed initial bio-inspired FSS.

There was a resonant frequency shift from 6.3 GHz to 6.0 GHz. This made the proposed bio-inspired FSS structure ideal for applications on Wi-Fi systems using Wi-Fi 6E standards. In this case, the filtering bandwidth starts at 5.0 GHz and ends at 6.75 GHz for a -10 dB insertion loss reference level. The important polarization independence property was maintained, as can be seen in the results.

Figure 8 shows the result obtained for the current distribution at 6.0 GHz. With the purpose of validating the result obtained for the proposed bio-inspired FSS structure, the simulated and measured results are shown in Figure 9. A good agreement can be seen in terms of resonance frequency at 6 GHz, the value of measured bandwidth was about 2.0 GHz starting from 4.86 GHz until 6.86 GHz.

In order to obtain a greater increase in the bandwidth, the structure was cascaded (forming the multilayer FSS structure) using a thick air layer between the single FSS structures (Figure 4) and, as can be seen from the results obtained, this procedure was positive. To obtain the results, the Scattering Matrix Technique was implemented using the Octave® software for equations 7 and 8. The numerical results for the multilayer or cascaded FSS, using different air layer thickness (d), are presented in Figures 10 – 13.

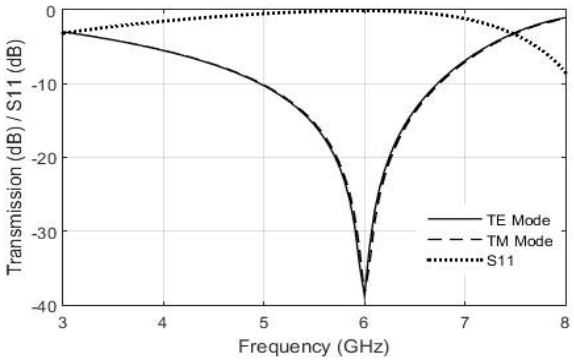

Figure 7. Simulated transmission coefficients for TE mode and TM mode and S_{11} for the proposed modified bio-inspired single FSS.

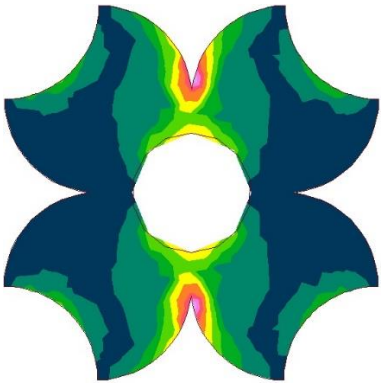

Figure 8. Current distribution, frequency at 6.0 GHz.

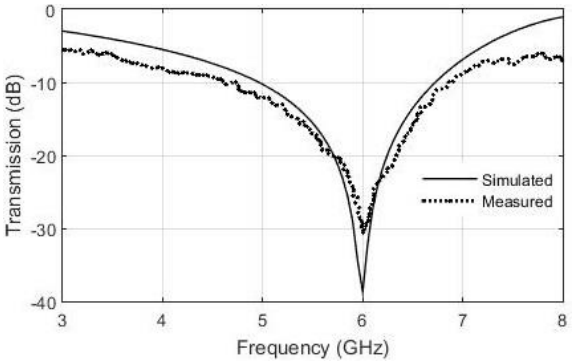

Figure 9. Simulated and measured transmission coefficients for the proposed modified bio-inspired single FSS.

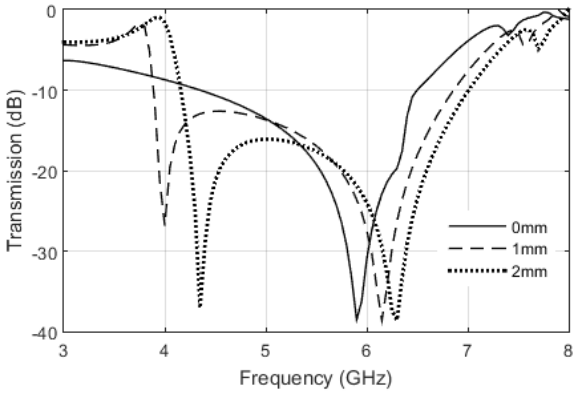

Figure 10. Simulated transmission coefficients for TE mode and TM mode for the multilayer FSS (*d* =0 mm, *d*=1 mm and *d*=2 mm).

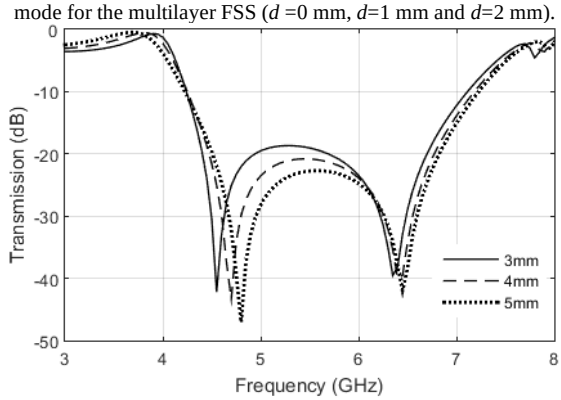

Figure 11. Simulated transmission coefficients for TE mode and TM mode for the multilayer FSS (*d* =3 mm, *d* = *4* mm and *d* = 5 mm).

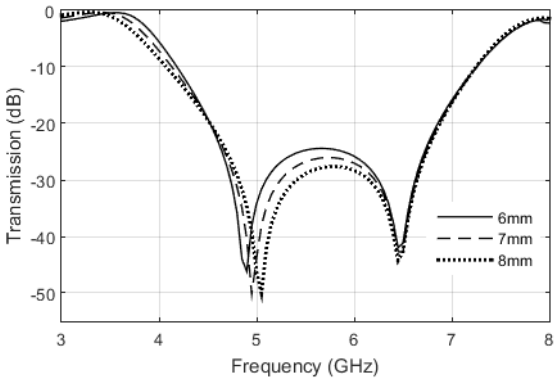

Figure 12. Simulated transmission coefficients for TE mode and TM mode for the multilayer FSS (*d* =3mm, *d*=4mm and *d*=5mm).

For these cases, it is possible to observe a considerable increase in the bandwidth.

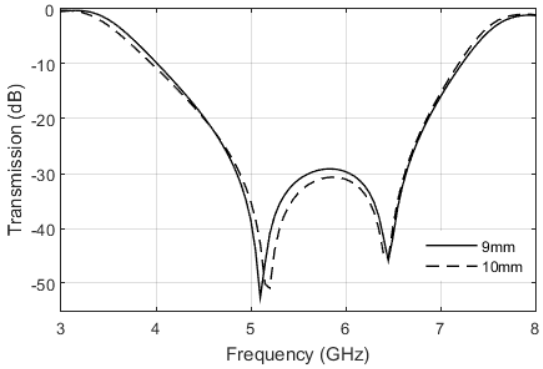

Figure 13. Simulated transmission coefficients for TE mode and TM mode for the multilayer FSS (*d* =9 and *d*=10mm).

This increase was about 1.4 GHz or 85.29%, when compared to the results shown in Figure 7 (single layer modified bio-inspired FSS structure), for the air layer thickness equal to 9 mm and 10mm. Now, it has bandwidth with filtering starting at 4.0 GHz and ending at 7.15 GHz for a -10 dB insertion loss reference level, totaling a value for this parameter equal to 3.15 GHz. Again, it can be highlighted that the multilayer FSS structure is also polarization-independent. As observed in the results presented, the proposed FSS structure is suitable for use in the frequency range of the proposed application. For Wi-Fi 6E, it has some 6.0 GHz spectrum access approaches with dynamic random spectrum access and contention-based protocols requiring access to multiple channels to maintain acceptable performance. Figure 14 shows the behavior of the bandwidth (stop-band filtering value) obtained as a function of parameter *d*, that is, as a function of the thickness of the air layer, for the multilayer FSS structure. Figure 15 shows all results together for comparison purposes.

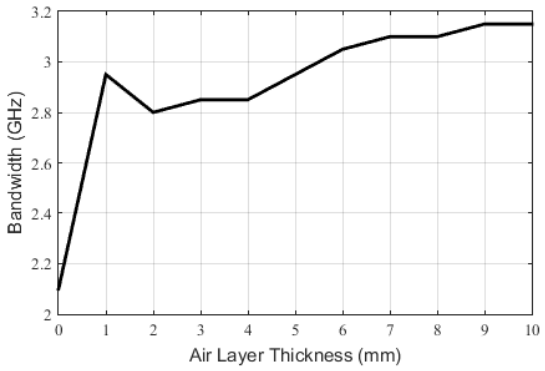

Figure 14. Bandwidth behavior as a function of the air layer thickness.

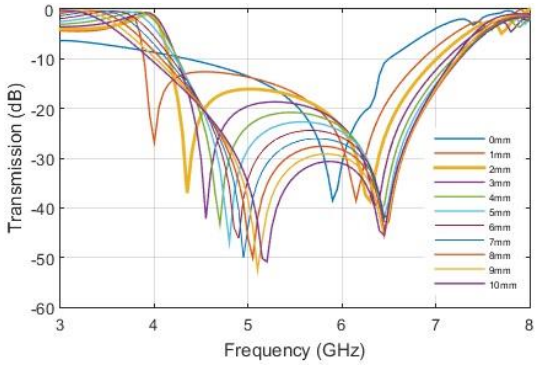

Figure 15. Bandwidth behavior as a function of the air layer thickness.

The technical conditions for a 6.0 GHz Very Low Power (VLP) device are, in terms of frequency band: US (proposed): 5.925 GHz -7.125 GHz, Europe (adopted): 5.945 GHz - 6.425 GHz, South Korea (adopted): 5.945 GHz - 6.425 GHz, Brazil (adopted): 5.925 GHz -7.125 GHz. The technical condition for 6.0 GHz Low Power Indoor-only (LPI) device: US (adopted): 5.925 GHz -7.125 GHz, Europe (adopted): 5.925 GHz -7.125 GHz, South Korea (adopted): 5.945 GHz - 6.425 GHz, Brazil (adopted): 5.925 GHz -7.125 GHz [28]. All frequency bands mentioned are within the bandwidth obtained for the multilayer bio-inspired FSS structure. In [32] a transparent and flexible patch antenna for Wi-Fi 6E applications is proposed with a measured frequency band of 5.87-7.04 GHz, where it is possible to verify that the proposed FSS structure can be used. In the work presented in [33], a small antenna for use in WLAN and Wi-Fi 6E on a narrow border laptop computer is proposed, for this case it is also possible to use the FSS proposed here. The FSS structure proposed in this work is of the same nature as previous works found in the literature of the area. One can cite the structure proposed in [34] where an active FSS with a butterfly-shaped aperture pattern is used. An FSS utilizing interdigital and supershape geometries with high angular and polarization stabilities is proposed [35]. In this case, the superformula (equation 1 used for the FSS format in Figures 2 and 3) proposed by Gielis in [31] is used to design the geometry of an FSS unit cell similar to shapes found in nature.

IV. CONCLUSION

A compact single and multilayer band-stop bio-inspired FSS is proposed in this paper. A simple modification on a bio-inspired element patch FSS was made. This modification allowed us to obtain a structure for Wi-Fi 6E applications. Due to the symmetrical shape of the element, the FSS structures (single and multilayer) have the advantage of polarization independence at Wi-Fi with 6 GHz frequency bands. As a proposal to continue this work, an investigation of the proposed multilayer FSS structure with a different substrate layer between the single FSS structures to observe the behavior in terms of transmission and reflection coefficients and bandwidths. The analysis of angular stability will be done in the future.

ACKNOWLEDGMENT

This work is supported by the Foundation for Research Support of the State of Bahia (FAPESB – Fundação de Amparo à Pesquisa do Estado da Bahia) and National Council for Scientific and Technological Development (CNPq – Conselho Nacional de Desenvolvimento Científico e Tecnológico).

REFERENCES

[1] T. K. Wu, Frequency Selective Surface and Grid Array. New York, NY: Wiley-Interscience, 1995.

[2] B. A. Munk, Frequency Selective Surface: Theory and Design. New York, NY: Wiley-Interscience, 2000.

[3] B. A. Munk, Finite Array and FSS. New York, NY: Wiley-Interscience, 2003.

[4] R. Mittra, C. H. Chan and T. Cwik, "Techniques for analyzing frequency selective surfaces-a review", Proceedings of the IEEE, vol. 76 (12), pp. 1593 – 1615, December 1988.

[5] J. H. Barton, C. R. Garcia, E. A. Berry, R. G. May, D. T. Gray and R.C. Rumpf, "All-Dielectric Frequency Selective Surface for High Power Microwaves", IEEE Transactions on Antennas and Propagation, vol. 62 (7), pp. 3652 – 3656, July 2014.

[6] A. L. P. S. Campos, A. G. d'Assunção and L. M. Mendonça, "Scattering by FSS on anisotropic substrate for TE and TM excitation", IEEE Transactions on Microwave Theory and Techniques, vol. 50 (1), pp. 72 – 76, January 2002.

[7] R. Dubrovka, J. Vazquez, C. Parini and D. Moore, "Multi-frequency and multi-layer frequency selective surface analysis using modal decomposition equivalent circuit method", IET Microwaves, Antennas & Propagation, vol. 3, pp. 492 – 500, April 2009.

[8] Q. Zhou, P. Liu, K. Wang, H. Liu and D. Yu, "Absorptive frequency selective surface with switchable passband", AEU - International Journal of Electronics and Communications, vol. 89, pp. 160 – 166, May 2018.

[9] D. B. Brito, A. G. d'Assunção, R. H. C. Maniçoba and X. Begaud, "Metamaterial inspired Fabry-Pérot antenna with cascaded frequency selective surfaces", Microwave and Optical technology Letters, vol. 55 (5), pp. 981 – 985, March 2013.

[10] H. Zhu, Y. Yu, X. Li and B. Ai, "A Wideband and High Gain Dual-Polarized Antenna Design by Frequency-Selective Surface for WLAN Application", Progress In Electromagnetics Research C (PIER C), vol. 54, pp. 57 – 66, October 2014.

[11] D. Gangwar, S. Das, R. L. Yadava and B. K. Kanaujia, "Circularly polarized inverted stacked high gain antenna with frequency selective surface", Microwave and Optical Technology Letters, vol. 58 (3), pp. 732 – 740, January 2016.

[12] Y. Cheng, W. Li and X. Mao, "Triple-Band Polarization Angle Independent 90º Polarization Rotator Based on Fermat's Spiral Structure Planar Chiral Metamaterial", Progress in Electromagnetics Research, vol. 165, pp. 35 – 45, July 2009.

[13] G. Yang, T Zhang, W Li and Q Wu, "A Novel Stable Miniaturized Frequency Selective Surface", IEEE Antennas and Wireless Propagation Letters, vol. 9, pp. 1018-1021, October 2010.

[14] T. Liu and Sumg-S. Kim, "High-capacitive frequency selective surfaces of folded spiral conductor arrays", Microwave and Optical Technology Letters, vol. 62, pp. 301-307, January 2020.

[15] R. Sivasamy, B. Moorthy, M. Kanagasabai, J. V. George, L. Lawrance and D. B. Rajendran, "Polarization-independent single-layer ultra- wideband frequency-selective surface", International Journal of Microwave and Wireless Technologies, vol. 9 (1), pp. 93 – 97, February 2017.

[16] F. Bagci, C. Mulazimoglu, S. Can, E. Karakaya, A. E. Yilmaz and B. Akaoglu, "A glass based dual band frequency selective surface for protecting systems against WLAN signals", AEU - International Journal of Electronics and Communications, vol. 82, pp. 426 – 434, December 2017.

[17] C. W. Lin, C. K. Shen, and T. L. Wu, "Ultracompact Via-Based Absorptive Frequency-Selective Surface for 5-GHz Wi-Fi With Passbands and High-Performance Stability", IEEE Transactions on Components, Packaging and Manufacturing Technology, vol. 8 (1), pp. 41 – 49, October 2017.

[18] U. Farooq, A. Iftikhar, M. F. Shafique, M. A. B. Abbasi, S. Clendinning, A. Fida, M. J. Mughal and M. S. Khan, "Ultraminiaturised Polarisation Selective Surface (PSS) for dual-band Wi-Fi and WLAN shielding applications", IET Microwaves, Antennas & Propagation, vol. 14 (13), pp. 1514 – 1521, October 2020.

[19] D. Ferreira, T. R. Fernandes, I. Cuiñas and R. F. S. Caldeirinha, "A dual-band single-layer frequency selective surface for Wi-Fi applications", in Proceedings of 2015 9th European Conference on Antennas and Propagation (EuCAP), April 2015.

[20] V. F. Barros, F. C. G. S. Segundo, A. L. P. S. Campos and S. G. Silva, "A Novel Simple Convoluted Geometry to Design Frequency Selective Surfaces for Applications at ISM and UNII Bands", Journal of Microwaves, Optoelectronics and Electromagnetic Applications, vol. 16 (2), pp. 553 – 563, June 2017.

[21] M.R. Chaharmir, J. Ethier and J. Shaker, "Design of a novel dual-band 2.4/5.5 GHz Frequency Selective Surface using loop elements", in Proceedings of the 6th International Conference on Metamaterials, Photonic Crystals and Plasmonics, August 2015.

[22] K. Mondal, "Bandwidth and gain enhancement of microstrip antenna by frequency selective surface for WLAN, WiMAX applications", Sādhanā, vol. 44, pp. 1 – 10, November 2019.

[23] A. Kumar, S. Dwari and G. P. Pandey, "A dual-band high-gain microstrip antenna with a defective frequency selective surface for wireless applications", Journal of Electromagnetic Waves and Applications, vol. 35, pp. 1637 – 1651, April 2021.

[24] J. N. Cruz, R. C. S. Freire, A. J. R. Serres, L. C. M. Moura, A. P. Costa and P. H. F. Silva, "Parametric Study of Printed Monopole Antenna Bioinspired on the Inga Marginata Leaves for UWB Applications", Journal of Microwaves, Optoelectronics and Electromagnetic Applications, vol. 16 (01), pp. 312 – 322, March 2017.

[25] P. F. S. Júnior, A.J. R. Serres, R. C. S. Freire, G. K. F. Serres, E. C. Gurjão, J. N. Carvalho and E. E. C. Santana, "Bio-Inspired Wearable Antennas", Wearable Technologies, IntechOpen, April 2018.

[26] M. D. S. Mesquita, A. G. D'Assunção, J. B. L. Oliveira and Y. M. V. Batista, "A New Conductive Ink for Microstrip Antenna and Bioinspired FSS Designs on Glass and Fiberglass Substrates", Journal of Microwaves, Optoelectronics and Electromagnetic Applications, vol. 18 (2), pp. 227 – 245, June 2019.

[27] "Wi-Fi 6E expands Wi-Fi® into 6 GHz", Wi-FI Alliance: www.wi-fi.org, January 2021.

[28] "Wi-Fi 6E and 6 GHz Update", Wi-Fi Alliance: www.wi-fi.org, March 2021.

[29] N. Gupta, J. Saxena and K. S. Bathia, "Design of Wideband Flower-Shaped Microstrip Patch Antenna for Portable Applications", Wireless Personal Communications, vol. 109, pp. 17 – 30, November 2019.

[30] J. Gielis, "A generic geometric transformation that unifies a wide range of natural and abstract shapes", American Journal of Botany, vol. 90, pp. 333-338, 2003.

[31] S. W. Lee, G. Zarrillo and C. L. Law, "Simple Formulas for Transmission Through Periodic Metal Grids or Plates", IEEE

Transactions on Antennas and Propagation, vol. 30 (5), pp. 904 – 909, 1982.

[32] T. D. Nguyen, Y. Lee and C. W. Jung, "Transparent and Flexible Patch Antenna Using MMF for Conformal Wi-Fi 6E Applications", Journal of Electromagnetic Engineering and Science, vol. 32, pp. 310-317, 2023.

[33] W. C. Jhang and J. S. Sun, "Small Antenna Design of Triple Band for Wi-Fi 6E and WLAN Applications in the Narrow Border Laptop Computer", International Journal of Antennas and Propagation, vol. 2021, pp. 1-8, 2021.

[34] J. H. Choi, J. Ahn, J. B. Kim, Y. C. Kim, J. Y. Lee and I. K. Oh, "An Electroactive, Tunable, and Frequency Selective Surface Utilizing Highly Stretchable Dielectric Elastomer Actuators Based on Functionally Antagonistic Aperture Control", Small, vol.12, pp. 1840-1846, 2016.

[35] A. Khajevandi and H. Oraizi, "Utilizing interdigital and supershape geometries for the design of frequency selective surfaces with high angular and polarizations stabilities", Scientific Reports, vol.12, pp. 1-13, 2022.